Identification of Adult Resistant Genes to Stripe Rust in Wheat from Southwestern China Based on GWAS and WGCNA Analysis

Liang Qiao

805497612@qq.com

Yunnan Agricultural University https://orcid.org/0000-0002-0600-3478

Xue Gao

Yunnan Agricultural University

Zhiqiang Jia

Yunnan Agricultural University

Xingchen Liu

Yunnan Agricultural University

Huiyutang Wang

Yunnan Agricultural University

Yixi Kong

Yunnan Agricultural University

Peng Qin

Yunnan Agricultural University

Baoju Yang

Yunnan Agricultural University https://orcid.org/0009-0006-9764-8066

Research Article

Keywords: GWAS, Resistant gene, RNA sequencing, Stripe rust, WGCNA

Posted Date: October 5th, 2023

DOI: https://doi.org/10.21203/rs.3.rs-3387252/v1

Version of Record: A version of this preprint was published at Plant Cell Reports on February 11th, 2024. See the published version at https://doi.org/10.1007/s00299-024-03148-4.

Abstract

Wheat stripe rust, which is caused by the wheat stripe rust fungus (Puccinia striiformis f. sp. tritici, Pst) is one of the world's most devastating diseases of wheat. Genetic resistance is the most effective strategy for controlling diseases. Although wheat stripe rust-resistance genes have been identified to date, only a few of them confer strong and broad-spectrum resistance. Here, the resistance of 335 wheat germplasm resources (mainly wheat landraces) from Southwestern China to wheat stripe rust was evaluated at the adult stage. Combined genome-wide association study (GWAS) and weighted gene co-expression network analysis (WGCNA) based on RNA sequencing from stripe rust resistant accession Y0337 and susceptible accession Y0402, five candidate resistance genes to wheat stripe rust (*TraesCS1B02G170200*, *TraesCS2D02G181000*, *TraesCS4B02G117200*, *TraesCS6A02G189300*, and *TraesCS3A02G122300*) were identified. The transcription level analyses showed that these five genes were significantly differentially expressed between resistant and susceptible accessions post inoculation with *Pst* at different times. These candidate genes could be experimentally transformed to validate and manipulate fungal resistance which is beneficial for development of the wheat cultivars resistant to stripe rust.

Key Message

In this study, genome-wide association studies combined with transcriptome data analysis were utilized to reveal potential candidate genes for stripe rust resistance in wheat, providing a basis for screening wheat varieties for stripe rust resistance.

Main text

Wheat stripe rust, which is caused by the wheat stripe rust fungus (*Puccinia striiformis* f. sp. *tritici*, *Pst*), is a major disease of wheat. Wheat stripe rust has been documented in more than 60 countries in Africa, Asia, Oceania, Europe, North America, and South America, and this disease results in major losses in wheat yield and quality on an annual basis (Li and Zeng. 2002; Guan et al.2020). Breeding varieties with resistance to wheat stripe rust are considered the most effective and environmentally friendly approaches for mitigating the deleterious effects of wheat stripe rust on wheat yield and quality (Chen 2005; Zhou et al. 2015).

Genes that confer resistance to wheat stripe rust can be divided into two types, all-stage resistance (ASR) and adult-plant resistance (APR) genes, depending on the stages in which they confer resistance to wheat stripe rust (Bouvet et al. 2022). ASR genes confer race specific resistance to wheat stripe rust and can provide resistance throughout the entire growth cycle. However, the loss of resistance to novel virulent pathogens can be accelerated when directional selection on wheat strains is strong; the resistance conferred by these genes thus tends to weaken three to five years after they are developed. APR genes are nonrace specific and are expressed only at the adult growth stage (Mourad et al. 2021); APR genes can also reduce the rate of mutation of wheat stripe rust pathogens, which can increase the persistence of resistance (Chen, 2013).

A total of 83 genes that promote resistance to wheat stripe rust have been identified in common wheat cultivars, local germplasm resources, and wild relatives to date, and these have been assigned permanent names; a total of 67 wheat stripe rust resistance genes have been assigned provisional names; and more than 300 quantitative trait loci (QTLs) have been identified (Li et al. 2020; Kumar et al. 2021; Huang et al. 2021). A total of 56 and 27 of the Yr genes that have been assigned permanent names are ASR genes and APR genes, respectively. Many studies have focused on exploring applications of these wheat stripe rust resistance genes; however, the only wheat stripe rust resistance genes that have been cloned to date include *Yr5*, *YrSP*, *Yr7*, *Yr10*, *Yr15*, *Yr18*, *Yr28*(*YrAS2388*), *Yr36*, *Yr46* and *YrU1* (Marchal et al. 2018; Liu et al. 2014; Klymiuk et al. 2018; Krattinger et al. 2009; Zhang et al. 2019; Fu et al. 2009; Moore et al. 2015; Wang et al. 2020;). Among the wheat stripe rust resistance genes that were successfully cloned, only three, *Yr18*, *Yr36*, and *Yr46*, had APR resistance.The breeding of wheat varieties with resistance to stripe rust at the adult stage is a major focus of current studies aimed at exploring the practical applications of these genes; the identification of genes that confer resistance to wheat stripe rust at the adult stage is facilitated resistance improvement.

Wheat landraces are important genetic resources that have been subjected to long periods of artificial and natural selection; these germplasm are well adapted to local environments and have greater production potential because they possess various genes of economic significance that are lacking in bred varieties (Shen et al. 2002).Successful control in over-summering areas is the key to achieving sustainable management of stripe rust in China (Wan et al. 2007). Yunnan is one of the trans-summer zones of stripe rust in China, and key zones of pathogen variability and racial virulence changes. Second, the unique highland climate of Yunnan has facilitated the genetic diversification of wheat varieties; the genetic diversity of local wheat landraces in Yunnan is high, and they comprise a unique component of China's wheat germplasm resources. There is thus a need to identify genes that confer resistance to wheat stripe rust in local landraces in Yunnan.

Here, the infection types of 335 wheat germplasm resources (mainly wheat landraces) to wheat stripe rust were evaluated. Genome-wide association studies (GWAS) based on genotyping by sequencing (GBS) were combined with weighted gene co-expression network analysis (WGCNA) of transcriptome data to identify candidate genes for resistance to wheat stripe rust. Our results could be leveraged in breeding efforts to develop wheat varieties with broad-spectrum and persistent resistance to wheat stripe rust.

Materials and Methods

Plant Material and Field Trials

A total of 335 wheat germplasm resources were provided by the Institute of Biotechnology and Germplasm Resources, Yunnan Academy of Agricultural Sciences, China, (Table 1), including 311 (93%) landraces and 24 (7%) cultivars.

Table 1
Summary of the ITs of the 335 wheat accessions in Yunnan at the adult stage

Trait	Environment	Min	Max	Mean	STDEV	CV
IT	19YN	0	9	1.25	2.35	1.88
	19XD	0	9	1.66	2.58	1.55
	20YN	0	9	5.27	2.83	0.54
	21YN	0	9	3.63	2.04	0.56
	22YN	0	9	3.67	1.86	0.51
	22XD	0	9	3.11	2.92	0.94
Min,minimum;Max,maximum;STDEV,standard deviation;CV,coefficient of variation						

Field trials were conducted to evaluate the resistance to wheat stripe rust at the adult stage. In the experimental field of Yunnan Agricultural University (25°13'N, 102°75'E), plants were subjected to stripe rust resistance under natural disease conditions during the growing seasons of 2018–2019, 2019–2020, 2020–2021, and 2021–2022; each of these field trials was referred to as 19YN, 20YN, 21YN, and 22YN, respectively. Plants were also characterized for stripe rust resistance under natural disease conditions during the 2018–2019 and 2021–2022 growing seasons at the Xundian County Modern Agriculture Research Site (25°20'N, 102°41'E), and these field trials were referred to as 19XD and 22XD, respectively. Field trials were thus conducted across a total of six environments: 19YN, 20YN, 21YN, 22YN, 19XD, and 22XD. All 335 accessions were planted in a randomized block design with three replications in each environment, sown in mid-October of each year and harvested in May of the following year, with each variety planted in 1m rows and 25 cm between each row. Mingxian 169 was planted every 20 rows as susceptible checks and surrounding the nursery to increase stripe rust pressure. When Mingxian 169 plants and other wheat varieties began to show clear signs of wheat stripe rust infection, the reaction types of all the wheat materials were characterized. Infection types (ITs) were scored using an ordinal scale of disease severity that has been previously developed to characterize the phenotypes of wheat plants following infection of wheat stripe rust pathogens; the ordinal scores range from 0 to 9, where 0 indicates resistance to infection, 1–3 indicate high resistance to moderate resistance, 4–6 indicate intermediate

resistance, and 7–9 indicate moderate to high susceptibility (Peterson et al. 1948; Wei et al. 2011). ITs of all wheat accessions were scored three to five times, with an interval of about 3 days between the two adjacent scores, and the highest IT score was retained as the final score in subsequent analysis.

Analysis of the Phenotypic Data

Violin plots were made using Prism software to visualize the distribution of ITs among wheat accessions. The maximum value, minimum value, mean, standard deviation (Stdev), and coefficient of variation (CV) were calculated for each IT. The Origin 2021 software was used to calculate the Pearson correlation coefficients of ITs between environments and make figures.

DNA Extraction and Genome Sequencing

Leaf samples were collected when wheat seedlings had reached the three-leaf stage. The cetyltrimethylammonium bromide method was used to extract genomic DNA. The genomic DNA was digested with restriction endonucleases Mse and Nla , and then barcodes were added to each sample and amplified for xxx cycles, then the barcoded samples were pooled and the desired fragments were selected for GBS library construction. The Illumina HiSeq sequencing platform was used to conduct 150-bp paired-end sequencing. Quality control analyses of the sequencing data were conducted, and BWA software (v0.7.17) was used to map the filtered sequencing data to the Chinese Spring genome (Triticum_aestivum.IWGSC.dna.toplevel.fa; V2). GATK (v4.1.4.0) software was used to identify genome-wide variants, and the “KNN” imputation algorithm in TASSEL (v5.2.60) software was used to impute missing variants in the original dataset (geno < 0.9). Plink (v1.90 b6.26) software was used to filter the variant loci with the parameters "maf > 0.05; geno < 0.4" (minor allele frequency > 0.05 and Missing genotype data < 0.4) to obtain high-quality single-nucleotide polymorphism (SNP) markers for the subsequent GWAS.

Population Structure, Phylogenetic, and Linkage Disequilibrium (LD) Analyses

Plink software was used to convert the data into .vcf format. Admixture (v1.3.0) software was used to conduct population genetic structure analyses with K-values ranging from 1 to 16. VCF2Dis (v1.46) (https://github.com/BGI-shenzhen/VCF2Dis) software was used to construct the pairwise distance matrix between all the samples in the .vcf file, and the iTOL server (https://itol.embl.de/) was used to build a phylogenetic tree via the neighbor-joining method.

LD decay analysis was performed on 335 wheat germplasm resources using PopLDdecay software with the parameter -MaxDist 100000 defining the maximum distance for LD decay estimation; LD decay plots were generated using the ggplot2 package in R software.

GWAS

A GWAS was conducted to determine associations between SNP markers and ITs in 335 wheat accessions from Yunnan at the adult stage. The software Tassel was used for the kinship matrix analysis. Tassel (v3.0.70)(Bradbury et al. 2007) software was used to convert the VCF format files into HMP format for association analysis. Genome-wide association analyses were performed separately for each environmental phenotype using both mixed linear model (MLM) (K + Q) and generalized linear model (GLM) approaches to broaden the initial screening of potential candidate genes. The MLM and GLM both yielded significant loci using the threshold $-\log_{10}(P) > 4.0$ (Li et al. 2012), and the CMplot package (https://github.com/YinLiLin/CMplot) was used to build Manhattan and QQ plots.

Selection of Varieties and RNA-seq

According to our analyses of the ITs of the 335 wheat accessions each year, Y0337, which was highly resistant to wheat stripe rust (average IT of 2), and Y0402, which was highly susceptible to wheat stripe rust (average IT of 9), were used in subsequent *Pst* inoculation experiments. These two wheat varieties were grown in an artificial culture room with the temperature maintained

between 16°C and 18°C during the day and between 12°C and 15°C at night; these plants were also subjected to a 14-h/10-h light/dark photoperiod. When wheat plants reached the second leaf stage, *Pst* strain CYR32 was mixed with talcum powder and inoculated on plant leaves at a ratio of 1:20, and the inoculated leaves were collected at 0h, 24h, 48h, 72h, 5d and 7d after inoculation as transcriptome sequencing samples.

The RNAprep Pure Plant kit DP411 (Tiangen Biotech, China) was used to isolate total messenger RNA. One μg of RNA from each sample was used to construct the complementary DNA (cDNA) library, and the insert fragments of the library were detected using a Qubit 3.0 fluorescence quantifier and Qsep400 high-throughput analysis system. Quantitative real-time polymerase chain reaction was used to determine the effective concentration of the library (effective library concentration > 2 nM) to ensure that the quality of the library was sufficiently high for subsequent analyses. Next, 150-bp paired-end sequencing was conducted using the Illumina NovaSeq 6000 sequencing platform. Clean reads were obtained by eliminating reads containing ploy-N, reads containing adapter and low-quality reads from raw reads. The Q30, GC content of clean reads were calculated simultaneously. The high-quality clean reads were mapped to Chinese Spring RefSeq v2.0 using software HISAT2 (Kim et al, 2015). Differentially expressed gene analysis was performed using DESeq2 (Love et al, 2014) software. Differentially expressed genes (DEGs) were obtained by comparing between samples at different periods after inoculation with stripe rust spores, and genes that also met padj ≤ 0.01 and $|\log2(\text{FoldChange})| \geq 1$ were considered as DEGs. GO (Gene Ontology) and KEGG (Kyoto Encyclopedia of Genes and Genomes) enrichment analyses were performed on the differential genes. GO and KEGG analyses were conducted using the R package ClusterProfiler (version 4.0.0) (Yu et al, 2012).

WGCNA

The R package WGCNA was used to analyze the weighted gene co-expression network (Langfelder and Horvath, 2008); fragments per kilobase of exon per million mapped fragments values were converted to $\log_2$ values to identify functional clusters or modules of highly co-expressed genes using the adjacency matrix. The following parameters were used to construct networks and detect modules: minimum module size, 30; minimum height for merging modules, 0.25; and weighted network, unsigned. Cytoscape software was used to visualize the co-expression networks (Shannon et al. 2003).

Fluorescence Quantitative Polymerase Chain Reaction (FQ-PCR) Validation

Six DEGs were randomly selected from each of the two comparison groups and subjected to FQ-PCR to validate the RNA-seq data. Three technical replicates were performed for each sample. The samples used in the FQ-PCR analyses were the same as those used for RNA-seq. An Aidlab Reverse Transcription Kit (TUREscript 1st Strand cDNA Synthesis Kit, Beijing, China) was used to synthesize cDNA. An Analytik Jena qTOWER 2.2 fluorescent quantitative PCR instrument (Jena, Germany) with 2× SYBR® Green Supermix (Biomarker Technologies, Beijing, China) was used to conduct FQ-PCR reactions. The $2^{-\Delta\Delta Ct}$ method was used to calculate the expression levels of genes (Livak and Schmittgen, 2001), and the Stdev of the three biological replicates was calculated. The *GAPDH* gene was used as the internal control (Li et al. 2015). GraphPad Prism 9.4.0 was used to create plots of the FQ-PCR and RNA-seq data.

Multi-omics Analysis

A multi-omics association analysis was conducted to reduce the number of candidate genes. The significant SNP loci obtained by genome-wide association analysis (GWAS) and the gene sets obtained by weighted co-expression network analysis (WGCNA) constructed from transcriptome data were compared and analyzed. Genes that could be identified in both gene sets were screened as candidate genes. The candidate genes were then further screened based on function predictions to finally obtain disease-resistant candidate genes.

Results

Phenotypes of Wheat Varieties Resistant to Wheat Stripe Rust

All phenotypes are provided in Supplementary Table S1, and the distribution of wheat stripe rust ITs is shown in Fig. 1A. The ITs of 335 wheat accessions in Yunnan at the adult stage ranged from 0 to 9, and the average IT was 3.10. These data suggest substantial variation in the ITs among the 335 wheat accessions in Yunnan. A total of 181 wheat varieties showed wheat stripe rust resistance at the adult stage (IT ≤ 6) in all six environments, and 60 varieties exhibited high and stable wheat stripe rust resistance (IT ≤ 3) at the adult stage. Pearson correlation coefficients of the wheat stripe rust ITs across environments were calculated. The Pearson correlation coefficients of ITs between field environments ranged from 0.33 to 0.69, and the average Pearson correlation coefficient was 0.54, suggesting that wheat stripe rust ITs were generally consistent across growing seasons and locations (Fig. 1B).

Distribution of Polymorphic SNP Sites

The 335 wheat accessions were genotyped by GBS and a total of 3,161,158 SNP loci were detected; these SNP loci were then filtered using the parameters “maf > 0.05 and geno < 0.4” which yielded a total of 226,206 high-quality SNP loci. The greatest number of markers was present in the B genome (125,531), the lowest number of markers was present in the D genome (9,190), and the number of markers present in the A genome (89,457) was intermediate between the number of markers present in the B and A genomes (Supplementary Table S2, Supplementary Fig. S1).

Analysis of Wheat Population Structure and LD

A total of 226,206 high-quality SNPs were used to conduct phylogenetic and population structure analyses. Admixture software (v1.3.0) was used to conduct the population structure analysis (K = 1–16), and the CV-validation error was lowest at a K-value of 4. Therefore, the wheat populations were divided into four subgroups according to different genotypes: Sub-1, Sub-2, Sub-3, and Sub-4 (Fig. 2A, B). Using phylogenetic tree analysis, the associated populations could be clustered into four subpopulations (Fig. 2C). Therefore, it is appropriate to classify the associated populations into four subpopulations.

The LD decay plot revealed that genome-wide r^2 decreased with physical distance (Fig. 2D). The LD decay distance at the whole-genome level was 94.8 Mb when LD ≤ 0.30 was used as the threshold, and the intersection of r^2 and the LD decay curve was used to infer the LD decay distance (Yao et al. 2019).

GWAS of Wheat Stripe Rust Resistance

The GLM and MLM models in TASSEL software were used to conduct a GWAS for wheat stripe rust resistance. GWAS significance thresholds were set using the Bonferroni correction of p-values. Both the MLM and GLM were used to identify significant loci ($-\log_{10}(P) > 4.0$), and the threshold for statistical significance was P = 1e-4.0. A GWAS for wheat stripe rust resistance revealed 88 SNP markers that were significantly associated with wheat stripe rust resistance on 21 chromosomes. The 88 SNPs were localized in 22 genomic regions, which were named 22 QTL: *QYr.ynau-1BS.1*, *QYr.ynau-1BS.2*, *QYr.ynau-1BL.1*, *QYr.ynau-1DS*, *QYr.ynau-1DL*, *QYr.ynau-2AL*, *QYr.ynau-2BL*, *QYr.ynau-2DS*, *QYr.ynau-3AS*, *QYr.ynau-3AL*, *QYr.ynau-3BL.1*, *QYr.ynau-3BL.2*, *QYr.ynau-4BS*, *QYr.ynau-4DL*, *QYr.ynau-5AL*, *QYr.ynau-5BL*, *QYr.ynau-6AS*, *QYr.ynau-6AL*, *QYr.ynau-6BS*, *QYr.ynau-7AS*, *QYr.ynau-7AL*,and *QYr.ynau-7BS*. These 22 QTLs were located on 16 chromosomes (1B, 1D, 2A, 2B, 2D, 3A, 3B, 4A, 4B, 4D, 5A, 5B, 6A, 6B, 7A, and 7B), explaining from 3.27–30.59% of the IT variation. Comparisons with previously reported QTL for *Yr* genes and physical locations identified 11 genes or QTL that may be identical or closely related to previously reported stripe rust resistance genes or QTL (Supplementary Table S3, Supplementary Fig. S2).

Transcriptome Analysis of DEGs

Transcriptome sequencing yielded 245.35 GB of clean data; the Q30 value of each sample ranged from 92.55–95.34%, and the GC content ranged from 52.26–57.20% (Supplementary Table S4). Comparison of samples at different time points following inoculation with *Pst* yielded 42,490 DEGs (Supplementary Table S5), of which samples Y0337 and Y0402 contained 23,123 deg together, 16,295 deg only in Y0337, and 3,072 DEG only in Y0402. The number of DEGs was higher in the 0 h vs. 24 h and 24 h vs. 48 h comparison groups than in the other comparison groups; the number of DEGs was also greater in all comparison groups of the variety resistant to wheat stripe rust Y0337 than in the variety susceptible to wheat stripe rust Y0402 (Fig. 3).

WGCNA

WGCNA was conducted on the RNA-seq data obtained from 36 samples of Y0337 and Y0402. The results of the hierarchical clustering analysis of the expression levels of genes in the Y0337 samples are shown in Fig. 4A. The threshold parameter β (β = 18) for the Y0337 samples was used to identify co-expression modules when the fitted curve was close to 0.9 (Fig. 4B); clustering analysis was then performed on the modules. After merging modules with similar expressions, a total of 20 modules were obtained (Fig. 4C). The number of genes in the modules ranged from 34 (the maroon module) to 4,834 (the turquoise module), and the expression relationships between the genes in each module are shown in Fig. 4D. Gene Ontology (GO) analysis was conducted on 20 modules. Each module contained genes that were significantly enriched in several GO pathways in the biological process, molecular function, and cellular component categories (Supplementary Fig. S3). The results of the GO analysis indicated that most of the genes identified via the WGCNA were involved in the following GO terms: “biological regulation” and “response to stimuli” in the biological process category; “membrane” and “organelle” in the cellular component category; and “catalytic activity”, “transporter activity”, “nucleic acid binding transcription factor activity”, and “enzyme regulator activity” in the molecular function category. In addition to these GO enrichments, genes in the Red module were enriched in the following GO terms in the molecular function category: “nutrient reservoir activity,” “molecular transducer activity”, “protein binding transcription factor activity”, and “receptor activity”. The genes in the Turquoise module were enriched in the following GO terms in the molecular function category: “molecular transducer activity”, “protein binding transcription factor activity”, “receptor activity”, and “guanyl-nucleotide exchange factor activity”. Genes in both the Red and Turqoise modules were disproportionately enriched in GO terms in the molecular function category compared with genes in the other modules. The genes in the Yellowgreen module were enriched in the following GO terms in the molecular function category only: “catalytic activity”, “transporter activity”, and “enzyme regulator activity”.

The results of the hierarchical clustering analysis of the expression levels of genes in Y0402 samples are shown in Fig. 5A. The threshold parameter β (β = 5) for the Y0402 samples was used to identify co-expression modules when the fitted curve was close to 0.9 (Fig. 5B); clustering analysis was then performed on the modules. After merging modules with similar expressions, a total of 19 modules were obtained (Fig. 5C). The number of genes in the modules ranged from 40 (LightsteelBlue1 module) to 3,432 (Turquoise module), and the expression relationships between the genes in each module are shown in Fig. 5D. GO analysis was conducted on 19 modules. Each module contained genes that were significantly enriched in several GO terms in the biological process, molecular function, and cellular component categories (Supplementary Fig. S4). The results of the GO analysis revealed that most of the genes identified via the WGCNA were involved in the following GO terms: “biological regulation” and “response to stimulus” in the biological process category; “membrane” and “organelle” in the cellular component category; and “catalytic activity”, “transporter activity”, “nucleic acid binding transcription factor activity”, and “enzyme regulator activity” in the molecular function category. In addition to these GO enrichments, genes in the Darkgreen module were enriched in the following GO terms in the molecular function category: “molecular transducer activity,” “receptor activity,” and “guanyl-nucleotide exchange factor activity.” Genes in the Darkgreen module were also disproportionately enriched in GO terms in the molecular function category compared with genes in the other modules.

FQ-PCR Validation

We conducted FQ-PCR analysis on six randomly selected DEGs from both the Y0337 and Y0402 samples to validate the RNA-seq data. The primer sequences are shown in Supplementary Table S6 Correlation analysis revealed a high correlation between the RNA-seq data and FQ-PCR data (R^2 of 0.7647), suggesting that our RNA-seq data were reliable (Supplementary Fig. S5; Supplementary Fig. S6).

Multi-omics Analysis

The significant SNPs identified by GWAS were compared with the candidate gene set identified by WGCNA, and finally, five candidate genes for wheat resistance to stripe rust were identified on chromosomes 1B, 2D, 3A, 4B and 6A (Fig. 6). These five candidate genes can be identified in both gene sets. (Fig. 6): a ribonuclease (RNase) gene (*TraesCS1B02G170200*), flavonol 3-

sulfotransferase-like gene (*TraesCS2D02G181000*), F-box protein genes (*TraesCS4B02G117200* and *TraesCS6A02G189300*), and cell wall-associated receptor kinase gene (*TraesCS3A02G122300*) (Table 2).

Table 2
Detailed information on the candidate genes involved in wheat stripe rust resistance in wheat

Gene name	Marker	Chromosome	Gene_start	Gene_end	NR_annotation	references
TraesCS1B02G170200	S1B_301973845	1B	302033116	302037366	ribonuclease 1-like [*Aegilops tauschii* subsp. *tauschii*]	Sun et al.,2021
TraesCS3A02G122300	S3A_96484556	3A	96682449	96685033	wall-associated receptor kinase-like 20 [*Aegilops tauschii* subsp. *tauschii*]	
TraesCS2D02G181000	S2D_125341639	2D	125343483	125345105	flavonol 3-sulfotransferase-like [*Aegilops tauschii* subsp. *tauschii*]	Yadav et al.,2016
TraesCS4B02G117200	S4B_135540506	4B	135812176	135815013	probable F-box protein At2g36090 [*Aegilops tauschii* subsp. *tauschii*]	Cobo et al. 2019
TraesCS6A02G189300	S6A_235470222	6A	237734651	237760058	GW2A [*Triticum aestivum*]	

Analysis of the Expression Patterns of Candidate Genes to Pst Infection

The results of the FQ-PCR analyses revealed that the above five candidate genes for wheat stripe rust resistance were differentially expressed at different time points in the variety resistant to wheat stripe rust (Y0337) and the variety susceptible to wheat stripe rust (Y0402) (Fig. 7), and the most significant changes in the expression of each candidate gene were observed 24 h after inoculation with *Pst*. The expression of *TraesCS1B02G170200* was down-regulated 24 h after *Pst* inoculation in Y0337, and the expression of this gene returned to a normal level after 48 h; the opposite expression pattern of this gene was observed in Y0402 over the same period. The expression of *TraesCS2D02G181000* was up-regulated and down-regulated in Y0337 24 h and 48 after *Pst* inoculation, respectively; the expression of this gene continued to decrease after *Pst* inoculation in Y0402. The expression of *TraesCS4B02G117200*, *TraesCS6A02G189300*, and *TraesCS3A02G122300* was significantly up-regulated 24 h after *Pst* inoculation in both Y0337 and Y0402, but the up-regulation of the expression of these candidate genes was much greater in Y0337 than in Y0402. These findings suggest that these five candidate genes for wheat stripe rust resistance responded to *Pst* inoculation, and the expression changes of these genes were most pronounced between 24 h and 48 h after *Pst* inoculation.

Analysis of the Gene Co-expression Network of Candidate Genes for Wheat Stripe Rust Resistance in Susceptible Varieties

A local regulatory network centered on the candidate genes identified by the multi-omics association analysis was constructed (Fig. 8). A total of 21 genes interacted with *TraesCS1B02G170200* in the modules identified via WGCNA. The *TraesCS4A02G489700* gene encodes LRR receptor-like serine/threonine protein kinase (At3g47570), and the other genes interacting with *TraesCS4A02G489700* mostly encode receptor kinases. Several of the interacting genes are directly or indirectly involved in the “plant–pathogen interaction” pathway (ko04626) according to the Kyoto Encyclopedia of Genes and Genomes (KEGG) analysis. A total of seven genes interacted with *TraesCS2D02G181000* in the Yellowgreen module, and the genes interacting with *TraesCS2D02G181000* were enriched in several GO terms in the molecular function category: “endonuclease activity” (GO:0004519), “hydrolase activity” (GO:0016787), “transferase activity,” and “transfer of acyl groups other than

aminoacyl groups" (GO:0016747). Among them, TraesCS4A02G489700 that interacted with candidate genes was associated with the flavonoid biosynthesis (ko00941) metabolic pathway. A local regulatory network map was built according to the connectivity of the 15 most significantly enriched genes in each module with the *TraesCS4B02G117200* and *TraesCS6A02G189300* genes. *TraesCS2A02G286200* was found to be enriched in "synthesis of the SCF ubiquitin ligase complex" (GO:0019005) and interacts with two candidate genes. Several genes were found to be directly or indirectly involved in "plant–pathogen interactions" (ko04626) according to KEGG analysis. The 30 genes with the highest connectivity to the *TraesCS3A02G122300* gene in the Darkgreen module were used to construct a local regulatory network map. GO analysis revealed that these genes were significantly enriched in the following GO terms: "positive regulation of innate immune response" (GO:0045089), "regulation of defense response to fungi" (GO:1900150), and "protein transport" (GO:0015031) in the biological process category. The gene *TraesCS5A02G232600* encodes the LRR receptor kinase SERK2. Multiple genes were directly or indirectly involved in "plant–pathogen interactions" (ko04626) according to KEGG analysis.

Discussion

Previous studies have shown that genetic correlations in populations increase the risk of detecting false positives in GWAS (Ali et al. 2020). Ideally, populations subjected to GWAS should possess sufficient genotypic and phenotypic diversity. In our study, population structure and a phylogenetic tree were conducted to analyze the structural characteristics of the sampled populations, and the results revealed large genetic differences among the 335 wheat accessions, indicating that they were ideal populations for GWAS. We obtained a total of 88 SNP markers that were significantly associated with wheat stripe rust resistance at the adult stage across 21 chromosomes using the GLM and MLM in TASSEL software.

Multiple correction approaches have been used to account for the detection of false positives in GWAS (Huang et al. 2013). However, the problem associated with the detection of false positives cannot be fundamentally solved regardless of the correction method used, and an overly conservative correction method can result in a large number of false negatives. Moreover, the contributions of loci with small effects to traits are often not statistically significant after multiple corrections because their signals are frequently difficult to distinguish from background noise. Several approaches have been used to circumvent these problems, including haplotype-based GWAS, gene-based GWAS, k-mer GWAS, GWAS using copy number variants, and the restricted two-stage multi-locus multi-allele GWAS approach, which is similar to haplotype-based GWAS (Huang et al. 2013; Schulthess et al. 2022; Zhao et al. 2022; He et al. 2017). WGCNA was first used as a complement to GWAS analysis to identify loci with small effects on bone mineral density (Farber, 2013). Previous studies have shown that the use of WGCNA to screen the large number of "notionally" significant genes from GWAS can enhance the identification of candidate genes. We conducted a GWAS and WGCNA to identify candidate genes for wheat stripe rust resistance; this approach permitted a large number of false-positive genes to be filtered, and we identified five genes that were highly correlated with wheat stripe rust resistance.

Although much research has been conducted on wheat stripe rust resistance genes, only a few resistance genes have been cloned, Although much research has been conducted on wheat stripe rust resistance genes, only a few resistance genes have been cloned, and of the stripe rust resistance genes that have been cloned to date, only *Yr18/Lr34/Sr57/Pm38* (Krattinger et al. 2019), *Yr36* (Fu et al. 2009), and *Yr46/Lr67/Sr55/Pm46* (Moore et al. 2015) have APR resistance.*Yr18/Lr34/Sr57/Pm38* has been documented in several wheat varieties in China, Italy, North America, South America, and Europe, and gene structure and function analysis have shown that this gene encodes an ATP-binding site-transferase (ABC); *Yr36* is derived from wild wheat and encodes a protein kinase, WKS1, which contains the START domain. Under high-temperature conditions, WKS1 might bind to lipids to prevent them from interacting with pathogens and activate the kinase, which eventually results in the death of pathogen cells and enhances disease resistance; *Yr46/Lr67/Sr55/Pm46* encodes a sugar transporter protein that promotes disease resistance by negatively regulating the uptake of glucose in infected leaves and reducing the carbon supply to the pathogen, which limits its growth. The genes that confer wheat stripe rust resistance at the adult stage lack a specific structural domain and have more complex structures than the main effector genes, which have conserved structural features characteristic of NBS-LRR genes. The five disease resistance candidate genes identified by our association analysis included the wheat RNase gene (TraesCS1B02G170200), flavonol 3-sulfotransferase-like gene (TraesCS2D02G181000), F-box protein genes (TraesCS4B02G117200 and TraesCS6A02G189300), and cell wall-associated receptor kinase gene

(TraesCS3A02G122300). These candidate genes are structurally and functionally different from previously cloned genes for stripe rust resistance at the adult stage and will help provide new ideas for future studies to identify new genes for stripe rust resistance in wheat.

The *TraesCS1B02G170200* gene is located within the *QYr.ynau-1BL.1* genomic region on chromosome 1B and has RNase T2 activity (GO:0033897). This gene is a member of the RNase T2 family, and it was annotated as wheat RNase 1-like according to the non-redundant (NR) library. In rice, the RNase T2 protein family comprises several members, which are named RNS1–RNS8. The RNase T2 family has been reported to play a key role in the response to drought and in the regulation of the phosphate cycle; according to the gene expression data, RNS4 might be involved in plant immune responses. Gao et al. (2018) successfully cloned RNS1–RNS6 using the Nihon Haru reference genome and characterized the interactions of RNS1, RNS2, RNS3, RNS4, RNS5, and RNS6 with other proteins. RNS1–RNS5 interact with SCRE2. A previous experiment has shown that some RNase T2 protein family members are involved in the immune response in tobacco. The results of this experiment also demonstrated that some members of the RNase T2 family can inhibit cell death induced by BAX and INF1 (Gao et al. 2018). In our study, *TraesCS1B02G170200* was classified in the Red module in the samples showing wheat stripe rust resistance by WGCNA, and this gene was significantly enriched in the following KEGG pathways: “ABC transporters”, “plant hormone signal transduction”, “flavonoid and flavonol biosynthesis”, and “plant-pathogen interactions” (Supplementary Fig. S7A). These metabolic pathways are mostly involved in plant stress responses. The ABC transporter protein family is involved in a series of plant life activities by transporting various substrates, among which ABCG plays an important role in metabolite and hormone transport, stress in adversity, and the secretion of secondary metabolites (Tang et al. 2023). Phytohormone signaling plays an important role in plant disease resistance and defense. Yan et al. used a combination of phytohormones to improve potato late blight resistance (Yan et al. 2023). Plant flavonoids respond to various types of stresses, which can effectively improve the tolerance and resistance of plants to stress (Ge et al. 2023). Previous studies indicate that wheat ribonuclease 1-like functional genes might be involved in the response to wheat stripe rust. Meanwhile, in an experiment to characterize the stripe rust resistance gene YrXK in the Chinese wheat line Xike01015, Sun et al. found that TraesCS1B02G170200.1 expression was slightly down-regulated after inoculation of CYR33 at the seedling stage of Xike01015, which was consistent with our characterization results (Sun et al. 2022).This candidate gene might play a negative regulatory role in the defense response according to differences in its expression in samples varying in wheat stripe rust resistance.

The *TraesCS2D02G181000* gene is located within the *QYr.ynau-2DS* genomic region on chromosome 2D. This candidate gene, which was enriched in the GO term “sulfotransferase activity” (GO:0008146), was annotated as flavonol 3-sulfotransferase-like. A previous study of the defense mechanism of a near-isogenic line of wheat, WL711 + Lr57, which possesses the leaf rust resistance gene Lr57 and the susceptible genotype WL711, has shown that flavonoid biosynthesis is involved in the responses of plants to various types of stress (Yadav et al. 2016), and sulfotransferase plays a key role in flavonoid biosynthesis by catalyzing the binding of sulfate to flavonoids and flavonols using 3'-phosphoadenosine 5'-phosphosulfate as a sulfate donor. TraesCS2D02G181000 was classified in the Yellowgreen module of the samples with wheat stripe rust resistance by the WGCNA; this gene was significantly enriched in the following KEGG pathways: “phosphatidylinositol signaling system,” “protein export,” “cysteine and methionine metabolism,” and “flavonoid biosynthesis” (Supplementary Fig. S7B). Phosphatidylinositol signaling plays an important role in plant stress resistance. Wang et al. analyzed the importance of phosphatidylinositol signaling in the early stages of drought stress (Wang et al. 2022). Gai et al showed that cysteine and methionine have regulatory effects on the growth of many plant pathogenic fungi (Gai et al. 2020). Flavonoid chemosynthetic compounds play an important role in plant disease resistance, and Li studies suggest that flavonoid biosynthesis may dominate resistance to stem ulcer disease in pepper (Li et al. 2021); this gene plays an important role in flavonoid biosynthesis according to the network interaction analysis. The expression of the TraesCS2D02G181000 gene was up-regulated in the variety showing wheat stripe rust resistance and down-regulated in the variety susceptible to wheat stripe rust 24 h after inoculation with *Pst*, suggesting that this candidate gene might play a key role in mediating resistance to wheat stripe rust.

TraesCS4B02G117200 and *TraesCS6A02G189300* are located within the *QYr.ynau-4BS* genomic region on chromosome 4B and the *QYr.ynau-6AS* genomic region on chromosome 6A, respectively, and are annotated as F-box proteins (At2g36090) and GW2A proteins, respectively, according to NR libraries. These genes were classified in the Turquoise module in the variety showing wheat stripe rust resistance according to the WGCNA, and this gene was significantly enriched in the following KEGG pathways:

“ABC transporter”, “phosphatidylinositol signaling system”, “plant hormone signal transduction”, “ubiquitin mediated proteolysis”, and “plant-pathogen interaction” (Supplementary Fig. S7C). Previous studies have shown that F-box proteins play a role in regulating the responses to various types of stress in plants, especially biotic stress responses; F-box proteins often regulate disease resistance through their effects on the jasmonic acid and salicylic acid pathways (Austin et al. 2002). During the fine localization of Lr46/Yr29/Sr58/Pm39/Ltn2 genes that promote disease resistance at the adult stage, Cobo et al (2019) identified TraesCS1B01G453800 in the chromosome 1BL annotation, which encodes an F-box protein that may promote disease resistance during the adult stage (Cobo et al. 2019). In barley (Hordeum vulgare) and tobacco, SGT1, a protein associated with R gene stimulation for disease resistance, was identified, and this protein directly binds to and activates the SCF complex, activates growth hormone and jasmonic acid signaling, and enhances plant disease resistance (Azevedo et al. 2002; Austin et al. 2002; Llorente et al. 2008). The F-box protein is a key component of the SCF complex that is responsible for recognizing target substrate proteins that are degraded. TraesCS6A02G189300 encodes a ubiquitin-protein ligase E3, and F-box proteins mostly regulate the response to wheat stripe rust via the SCF complex ubiquitin ligase E3-mediated degradation of target proteins by ubiquitinated proteins. According to the results of the network interaction analysis, the TraesCS2A02G286200 gene is involved in the synthesis of the SCF ubiquitin ligase complex (GO:0019005) and interacts simultaneously with two candidate genes, TraesCS4B02G117200 and TraesCS6A02G189300. The TraesCS6A02G189300 gene may be involved in the regulation of the response to wheat stripe rust through the regulation of the synthesis of ubiquitin protein ligase E3. The GWAS and WGCNA suggested that TraesCS4B02G117200 and TraesCS6A02G189300 might be jointly involved in regulating the response of wheat plants to stress via the SCF complex.

TraesCS3A02G122300 is located in the *QYr.ynau-3AS* genomic region on chromosome 3A, and this candidate gene is annotated as wall-associated receptor kinase 20 according to the NR library. This gene was classified in the Darkgreen module by the WGCNA of the variety that was susceptible to wheat stripe rust, and it was significantly enriched in the following KEGG pathways: “ABC transporters,” “plant hormone signal transduction”, “flavone and flavonoid biosynthesis”, “serine and threonine metabolism”, and “plant-pathogen interaction” (Supplementary Fig. S7D). The wall-associated receptor kinase 25 (OsWAK25) of the cell wall-associated kinase family positively regulates the resistance of rice to *Xanthomonas campestris pv. Oryzae* and *Magnaporthe grisea* and negatively regulates resistance to *Rhizoctonia solani* and *Cochliobolus miyabeanus* (Harkenrider et al. 2016). OsWAK25 has a transmembrane receptor protein serine/threonine kinase activity function, which is consistent with the enrichment of KEGG Pathway function in the Darkgreen module. The results of the network interaction analysis revealed that this gene interacted with TraesCS5A02G232600, which encodes the LRR receptor kinase SERK2. The expression of candidate genes was upregulated in both wheat stripe rust resistant accession Y0337 and susceptible accession Y0402 24 h after inoculation with the stripe rust fungus; however, the expression of these candidate genes was up-regulated to a much greater degree in the variety showing wheat stripe rust resistance than in the variety susceptible to wheat stripe rust. Our findings indicate that wheat wall-associated receptor kinase 20 might be directly or indirectly involved in regulating disease resistance.

Conclusion

A GWAS of the wheat stripe rust resistance at the adult stage of 335 wheat germplasm resources (mainly wheat landraces) was conducted using GBS technology. Transcriptome sequencing and WGCNA were conducted on varieties showing high wheat stripe rust resistance and high susceptibility to wheat stripe rust. We identified a total of 88 significant SNP loci according to the results of the GWAS and WGCNA of these selected varieties, as well as five candidate genes that were highly associated with wheat stripe rust resistance, including TraesCS1B02G170200, which encodes an RNase; TraesCS2D02G181000, which encodes the flavonol 3-sulfotransferase-like protein; TraesCS4B02G117200 and TraesCS6A02G189300, which encode F-box proteins; and TraesCS3A02G122300, which encodes the cell wall-associated receptor kinase-like 20 protein. These candidate genes were found to be involved in several biological processes, including ribonucleic acid kinase metabolism, flavonoid biosynthesis, and the composition of the SCF complex. Functional analysis revealed that these five candidate genes were involved in regulating disease resistance in wheat via different metabolic pathways.

Integrated analyses of histological data provide an effective approach for identifying the candidate genes underlying complex traits. In this study, we used GWAS and WGCNA to identify candidate genes for wheat stripe rust resistance at the adult stage in

wheat landraces in Yunnan. Additional studies are needed to characterize the functions of these genes via overexpression assays, gene silencing, or gene editing. The results of our study provide valuable information on candidate genes for wheat stripe rust resistance at the adult stage in several wheat landraces in Yunnan. The findings of our study will aid future studies aimed at genetically improving the resistance of wheat varieties to wheat stripe rust.

Declarations

Author contribution statement

Liang Qiao and Baoju Yang: Conceptualization and writing draft, review & editing. **Xue Gao and Zhiqiang Jia:** Data Collection. **Xingchen Liu, Huiyutang Wang and Yixi Kong:** Investigation. **Peng Qin:** Data curation. All authors contributed to the article and approved the submitted version.

Funding

This research was sponsored by grants from the National Natural Science Foundation of China (32160481), Yunnan Youth Talent Support Program, China.

Data availability

The original contributions presented in the study are publicly available. The data can be accessed at the following link: https://www.ncbi.nlm.nih.gov/search/all/?term= PRJNA938609.

Conflict of interest On behalf of all authors, the corresponding author states that there is no conflict of interest.

Ethics approval and consent to participate Not applicable.

Consent to participate Not applicable.

Consent for publication Not applicable.

References

1. Ali N, Li D, Eltahawy MS et al (2020) Mining of favorable alleles for seed reserve utilization efficiency in Oryza sativa by means of association mapping. BMC Genet 21:4
2. Austin MJ, Muskett P, Kahn K et al (2002) Regulatory role of SGT1 in early R gene-mediated plant defenses. Science 295:2077–2080
3. Azevedo C, Sadanandom A, Kitagawa K et al (2002) The RAR1 interactor SGT1, an essential component of R gene-triggered disease resistance. Science 295:2073–2076
4. Bouvet L, Percival-Alwyn L, Berry S et al (2022) Wheat genetic loci conferring resistance to stripe rust in the face of genetically diverse races of the fungus Puccinia striiformis f. sp. tritici. Theor Appl Genet 135:301–319
5. Bradbury PJ, Zhang Z, Kroon DE et al (2007) TASSEL: software for association mapping of complex traits in diverse samples. Bioinformatics 23(19):2633–2635
6. Chen XM (2005) Epidemiology and control of stripe rust [Puccinia striiformis f. sp. tritici] on wheat. Can J Plant Pathol 27:314–337
7. Chen XM (2013) Review article: High-temperature adult-plant resistance, key for sustainable control of stripe rust. Am J Plant Sci 4:608–627
8. Cobo N, Wanjugi H, Lagudah E, Dubcovsky J (2019) A high-resolution map of wheat QYr. ucw-1BL, an adult plant stripe rust resistance locus in the same chromosomal region as Yr29. 12:180055The plant genome

9. Farber CR (2013) Systems-level analysis of genome-wide association data. G3: Genes|. Genomes| Genet 3:119–129
10. Fu D, Uauy C, Distelfeld A et al (2009) A kinase-START gene confers temperature-dependent resistance to wheat stripe rust. Science 323:1357–1360
11. Gai Y, Li L, Ma H et al (2021) Critical role of MetR/MetB/MetC/MetX in cysteine and methionine metabolism, fungal development, and virulence of Alternaria alternata. Appl Environ Microbiol 87:e01911–e01920
12. Gao H, Fang AF, Sun XX (2018) Function of rice ribonuclease T2 protein family in disease resistance. Proceedings of the 2018 Annual Conference of the Chinese Society for Plant Pathology. China Agricultural Science and Technology Press. 449
13. Ge SB, Zan XN, Han WY, Li QY, Li X (2023) Research Progress on Plant Flavonoids Biosynthesis and Their Anti-stress Mechanism. Acta Horticulturae Sinica 50:209–224
14. Guan FN, Long L, Yao FJ et al (2020) Evaluation of resistance to stripe rust and molecular detection of important known Yr gene (s) of 152 Chinese wheat landraces from the Huang-huai-hai. Sci Agric Sin 53:3629–3637
15. Harkenrider M, Sharma R, Vleesschauwer DD et al (2016) Overexpression of rice wall-associated kinase 25 (oswak25) alters resistance to bacterial and fungal pathogens. PLoS ONE 11:e0147310
16. He J, Meng S, Zhao T et al (2017) An innovative procedure of genome-wide association analysis fits studies on germplasm population and plant breeding. Theor Appl Genet 130:2327–2343
17. Huang S, Liu S, Zhang Y et al (2021) Genome-wide wheat 55K SNP-based mapping of stripe rust resistance loci in wheat cultivar Shaannong 33 and their alleles frequencies in current Chinese wheat cultivars and breeding lines. Plant Dis 105:1048–1056
18. Huang Y, Kong X, Zhen Z, Liu J (2013) The comparison of multiple testing corrections methods in genome-wide association studies. Adv Psychol Sci 21:1874
19. Kim D, Langmead B, Salzberg SL (2015) HISAT: a fast spliced aligner with low memory requirements. Nat Methods 12(4):357–360
20. Klymiuk V, Yaniv E, Huang L et al (2018) Cloning of the wheat *Yr15* resistance gene sheds light on the plant tandem kinase-pseudokinase family. Nat communication 9:3735
21. Krattinger SG, Lagudah ES, Spielmeyer W et al (2009) A putative ABC transporter confers durable resistance to multiple fungal pathogens in wheat. Science 323:1360–1363
22. Kumar S, Bhardwaj SC, Gangwar OP et al (2021) Lr80: A new and widely effective source of leaf rust resistance of wheat for enhancing diversity of resistance among modern cultivars. Theor Appl Genet 134:849–858
23. Langfelder P, Horvath S (2008) WGCNA: an R package for weighted correlation network analysis. BMC Bioinformatics 9:1–13
24. Li H, Niu WH, Liu N et al (2015) Reference Gene Selection for RT-qPCR and Expression Analysis of TaSGR Gene in Defense Response of Wheat to Puccinia triticina. Plant Physiol Commun 51:642–648
25. Li J, Dundas I, Dong C et al (2020) Identification and characterization of a new stripe rust resistance gene *Yr*83 on rye chromosome 6R in wheat. Theor Appl Genet 133:1095–1107
26. Li MX, Yeung JM, Cherny SS, Sham PC (2012) Evaluating the effective numbers of independent tests and significant p-value thresholds in commercial genotyping arrays and public imputation reference datasets. Hum Genet 131:747–756
27. Li P, Ruan Z, Fei Z, Yan J, Tang G (2021) Integrated transcriptome and metabolome analysis revealed that flavonoid biosynthesis may dominate the resistance of Zanthoxylum bungeanum against stem canker. J Agric Food Chem 69:6360–6378
28. Li ZQ, Zeng SM (2002) Wheat Rust in China. China Agriculture Press, Beijing, pp 370–373
29. Liu W, Frick M, Huel R et al (2014) The stripe rust resistance gene *Yr10* encodes an evolutionary-conserved and unique CC–NBS–LRR sequence in wheat. Mol Plant 7:1740–1755
30. Livak KJ, Schmittgen TD (2001) Analysis of relative gene expression data using real-time quantitative PCR and the $2^{-\Delta\Delta CT}$ method. Methods 25:402–408 d

31. Llorente F, Muskett P, Sánchez-Vallet A et al (2008) Repression of the auxin response pathway increases Arabidopsis susceptibility to necrotrophic fungi. Mol Plant 1:496–509
32. Love MI, Huber W, Anders S (2014) Moderated estimation of fold change and dispersion for RNA-seq data with DESeq2. Genome Biol 15(12):1–21
33. Marchal C, Zhang J, Zhang P et al (2018) BED-domain-containing immune receptors confer diverse resistance spectra to yellow rust. Nat Plant 4:662–668
34. Moore JW, Herrera-Foessel S, Lan C et al (2015) A recently evolved hexose transporter variant confers resistance to multiple pathogens in wheat. Nat Genet 47:1494–1498
35. Mourad AMI, Abou-Zeid MA, Eltaher S, Baenziger PS, Börner A (2021) Identification of candidate genes and genomic regions associated with adult plant resistance to stripe rust in spring wheat. Agronomy 11:2585
36. Peterson RF, Campbell AB, Hannah AE (1948) A diagrammatic scale for estimating rust intensity on leaves and stems of cereals. Can J Res 26:496–500
37. Schulthess AW, Kale SM, Liu F et al (2022) Genomics-informed prebreeding unlocks the diversity in genebanks for wheat improvement. Nat Genet 54:1544–1552
38. Shannon P, Markiel A, Ozier O et al (2003) Cytoscape: a software environment for integrated models of biomolecular interaction networks. Genome R esearch 13:2498–2504
39. Shen YH, Wang HQ, Yang TY, Zhang H, Huang XG (2002) Evolvement of genetic diversity of spring wheat varieties in gansu and qinghai provinces. Acta Bot Boreali-occidentalia Sinica 22:7–16
40. Sun C, Liu Y, Li Q et al (2021) Rapid identification of a stripe rust resistance gene YrXK in Chinese wheat line Xike01015 using specific locus amplified fragment (SLAF) sequencing. Plant disease. 10.1094/PDIS-12-20-2648-RE
41. Tang TX, Kong WP, Ren KL, Cheng H (2023) Advances in functional studies of plant ABC transporter proteins. Acta Agriculturae Boreali-Occidentalis Sinica 32:1–10
42. Wan AM, Chen XM, He ZH (2007) Wheat stripe rust in China. Aust J Agric Res 58:605–619
43. Wang H, Zou S, Li Y, Lin F, Tang D (2020) An Ankyrin-Repeat And WRKY-Domain-Containing Immune Receptor. Confers Stripe Rust Resistance In Wheat
44. Wang X, Deng Y, Gao L et al (2022) Series-temporal transcriptome profiling of cotton reveals the response mechanism of phosphatidylinositol signaling system in the early stage of drought stress. Genomics 114:110465
45. Wei GR, Han DJ, Zhao J et al (2011) Identification and evaluation of adult plant resistance to stripe rust in wheat germplasms. J Triticeae Crops 2:376–381
46. Yadav IS, Amandeep S, Satinder K et al (2016) Comparative Temporal Transcriptome Profiling of Wheat near Isogenic Line Carrying Lr 57 under Compatible and Incompatible Interactions. Frontiers in Plant Science 7, 1943
47. Yan W, Jian Y, Duan H et al (2023) Dissection of the Plant Hormone Signal Transduction Network in Late Blight-Resistant Potato Genotype SD20 and Prediction of Key Resistance Genes. Phytopathology 113:528–538
48. Yao F, Zhang X, Ye X Characterization of molecular diversity and genome-wide association study of stripe rust resistance at the adult plant stage in Northern Chinese wheat landraces. BMC genetics, 20(1), 1–16., Yu G, Wang LG, Han Y, He QY et al (2019) 2012. clusterProfiler: an R package for comparing biological themes among gene clusters. Omics: a journal of integrative biology, 16(5), 284–287
49. Zhang C, Huang L, Zhang H et al (2019) An ancestral NB-LRR with duplicated 3'UTRs confers stripe rust resistance in wheat and barley. Nat Commun, 10(1)
50. Zhao Y, Gao J, Guo X et al (2022) Gene-Based Genome-Wide Association Study Identified Genes for Agronomic Traits in Maize. Biology 11:1649
51. Zhou XL, Zhai GM, Huang LL, Han DJ, Kang ZS (2015) Evaluation of resistance to stripe rust in eighty abroad spring wheat germplasms. Scientia Agricultura Sinica 08:1518–1526

Figures

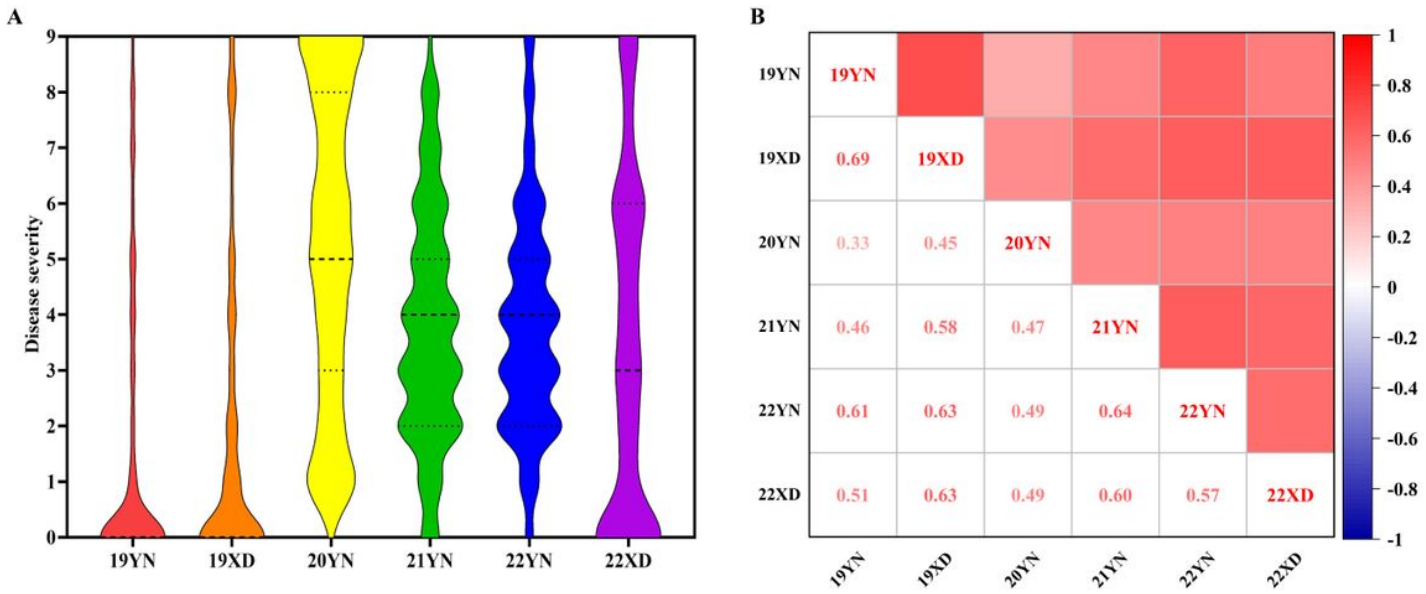

Figure 1

(A) Plot of the ITs of the wheat accessions across the six environments. (B) Heatmap of the Pearson correlation coefficients among the ITs across the six environments. Environments refer to combinations of growing seasons and locations: 19YN, 20YN, 21YN, and 22YN refer to the 2018–2019, 2019–2020, 2020–2021, and 2021–2022 growing seasons at the Experimental Field of Yunnan Agricultural University, respectively, and 19XD and 22XD refer to the 2018–2019 and 2021–2022 growing seasons at Xundian Dahe Bridge Research Base, respectively.

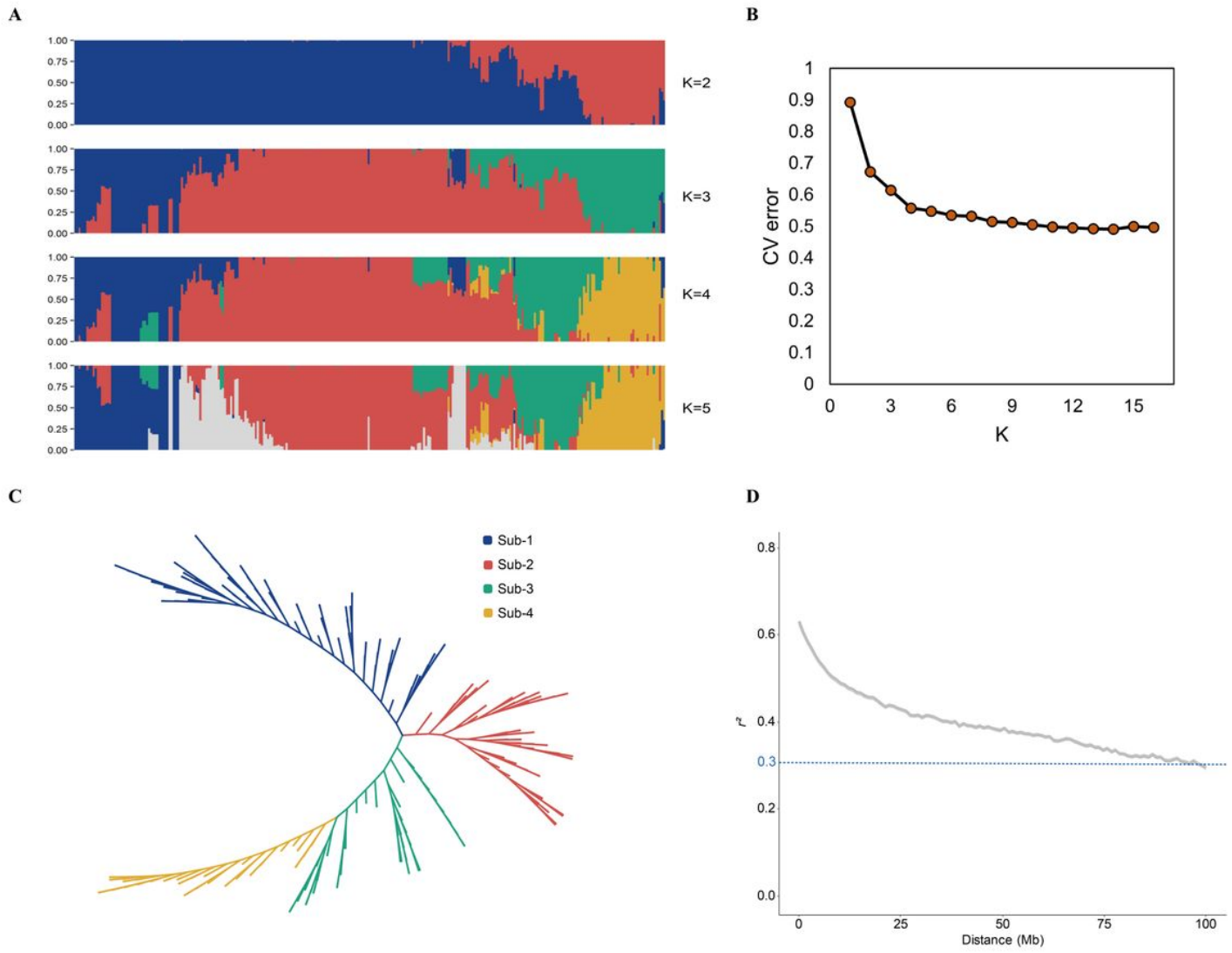

Figure 2

(A) Subgroups inferred by the structure analysis. (B) CV error of K-values from 1 to 16 in the structure analysis. (C) Neighbor-joining tree of all wheat landraces. (D) LD decay plot. The horizontal blue dashed line indicates the standard critical r^2. The intersection of the LD decay curve and the threshold limit (0.30) occurs at 94.8 Mb.

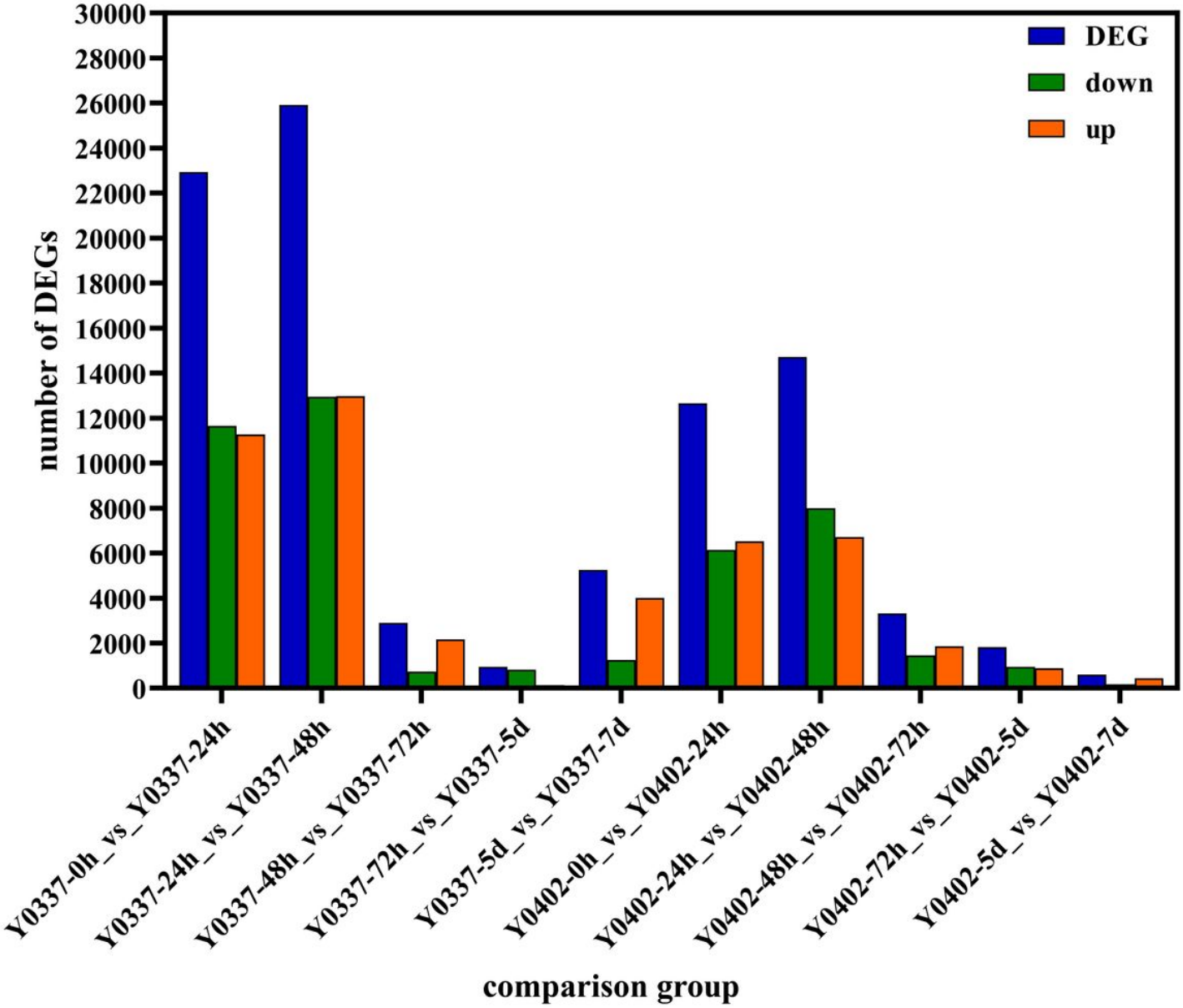

Figure 3

The number of up-regulated, down-regulated, and total DEGs in different comparison groups at various time points following *Pst* inoculation in a wheat variety resistant to wheat stripe rust (Y0337) and a wheat variety susceptible to wheat stripe rust (Y0402).

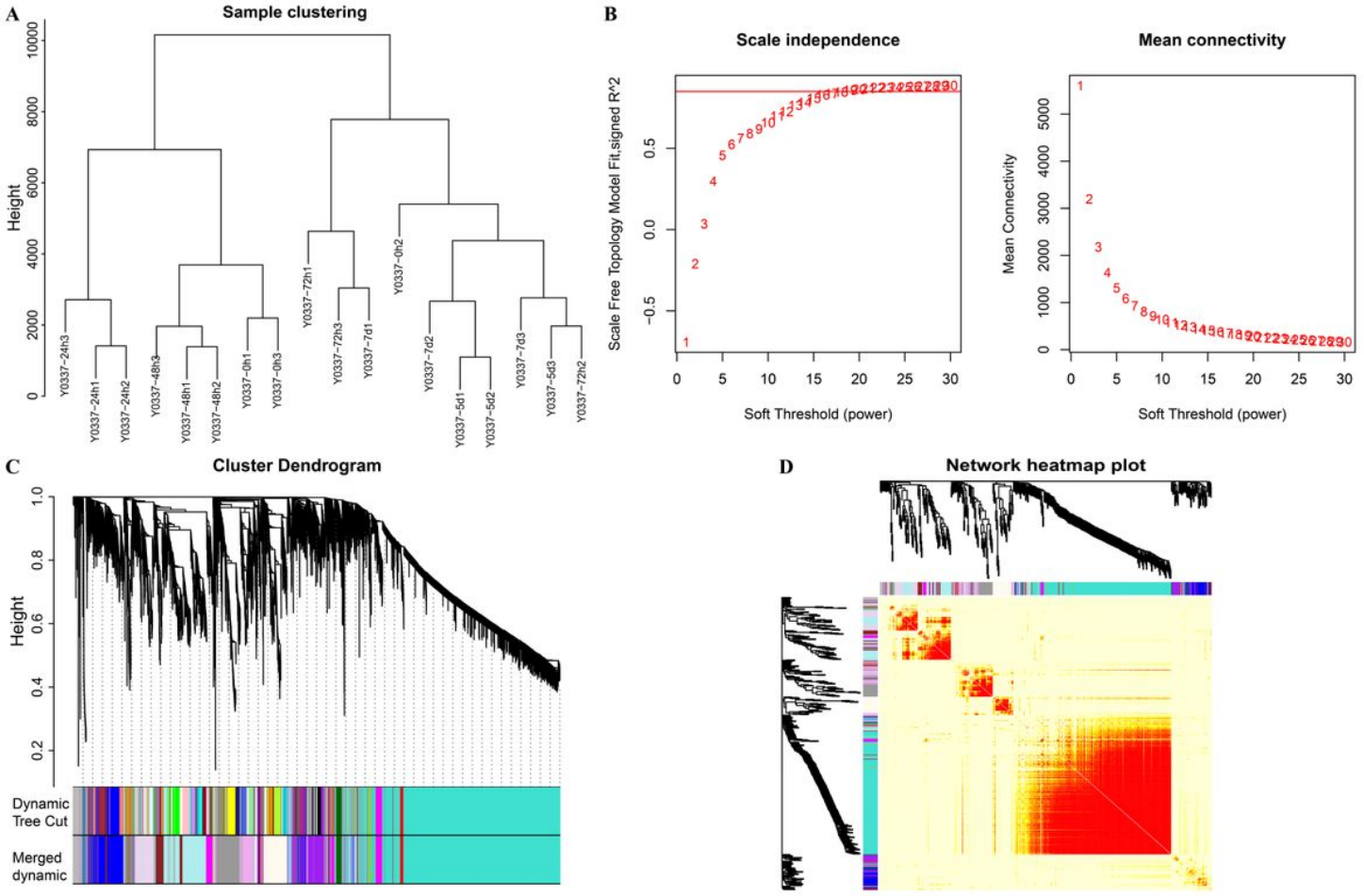

Figure 4

(A) Clustering of Y0337 samples. (B) Plots of the soft threshold vs. scale independence and mean connectivity. (C) Tree cluster diagram of the identified modules. (D) Heat map of the identified modules.

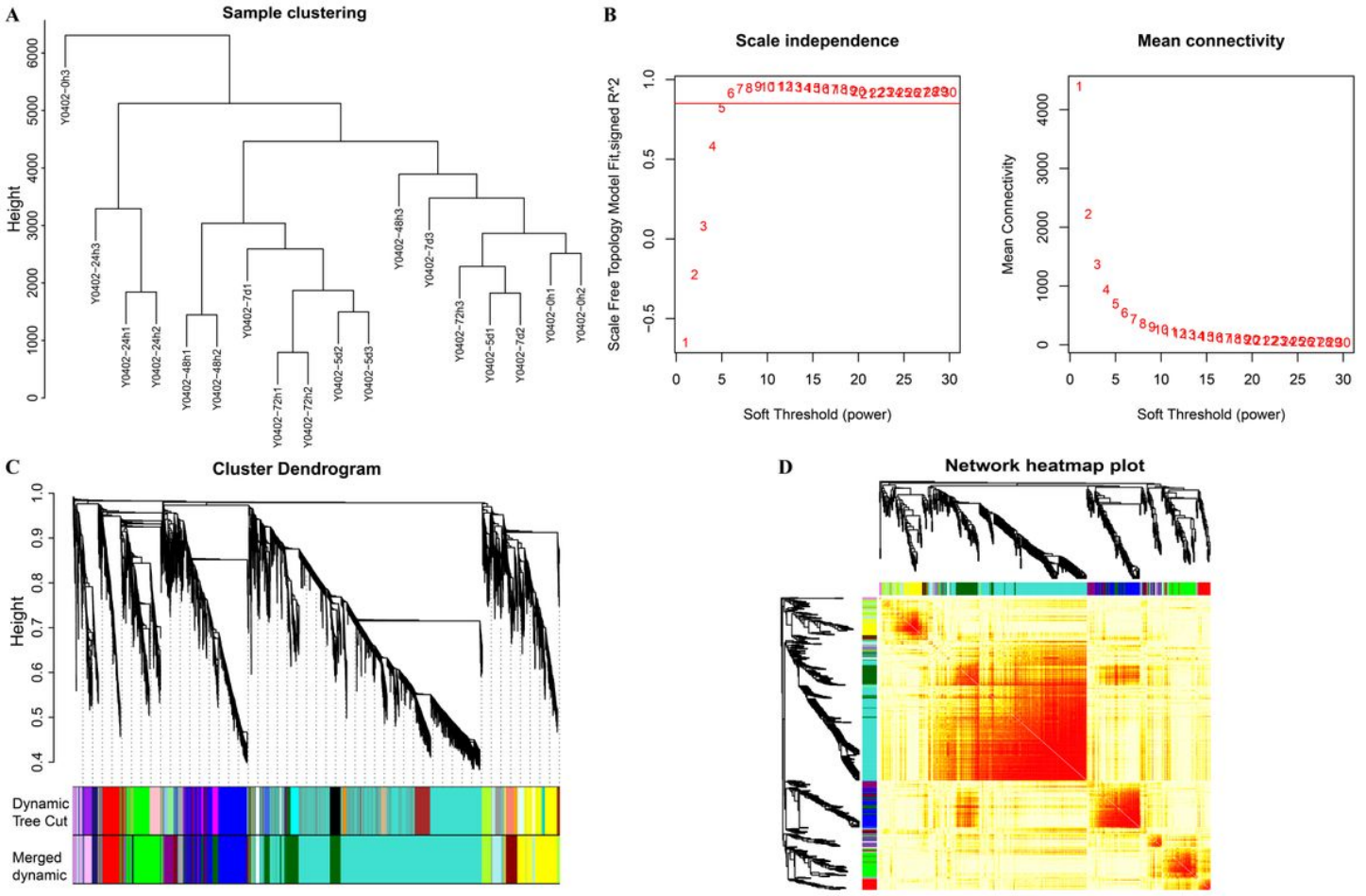

Figure 5

(A) Clustering of Y402 samples. (B) Plots of the soft threshold vs. scale independence and mean connectivity. (C) Tree cluster diagram of the identified modules. (D) Heat map of the identified modules.

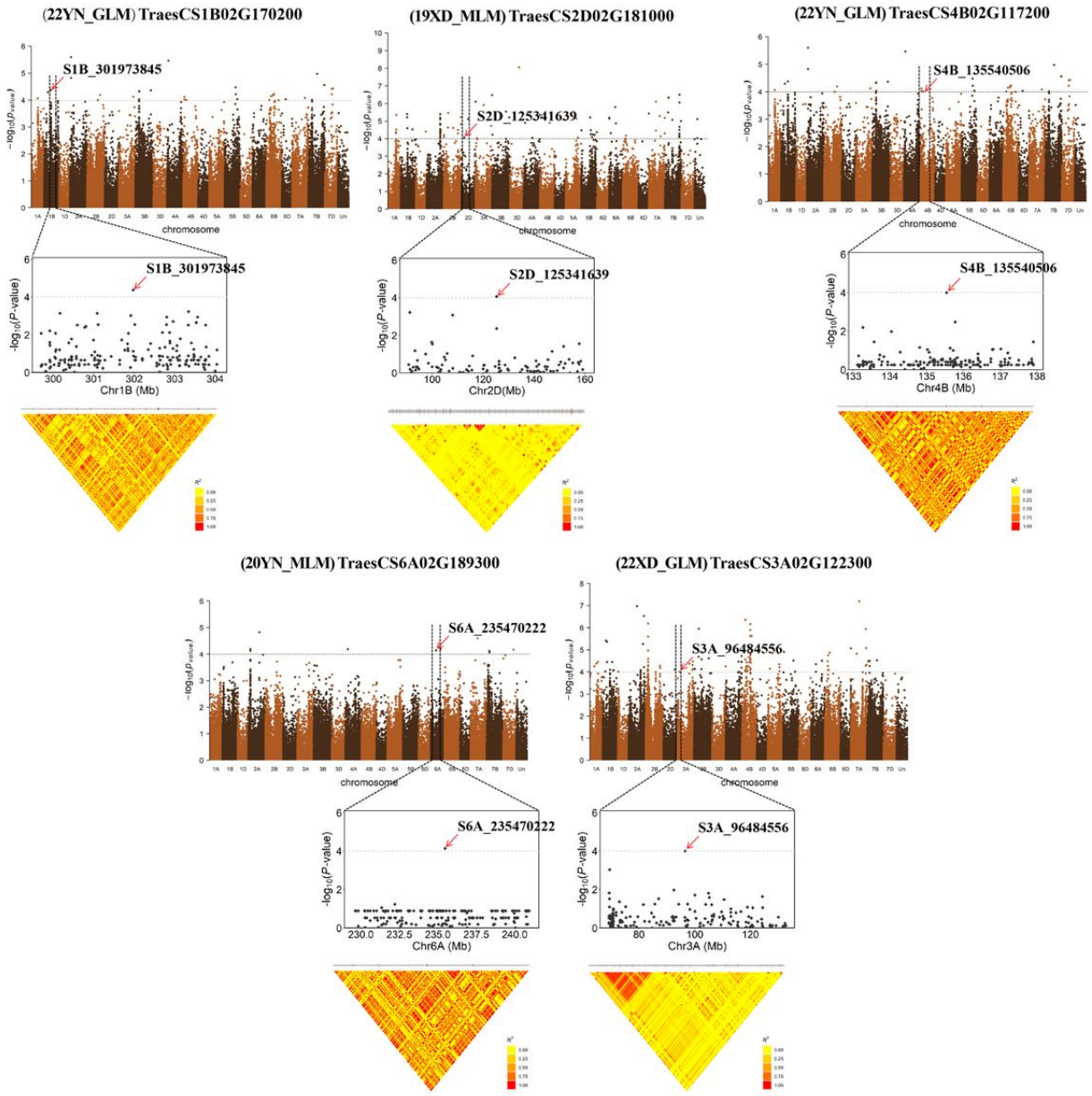

Figure 6

Local Manhattan plot of the five candidate genes identified via GWAS and WGCNA: *TraesCS1B02G170200*, *TraesCS2D02G181000*, *TraesCS4B02G117200*, *TraesCS6A02G189300*, and *TraesCS3A02G122300*.

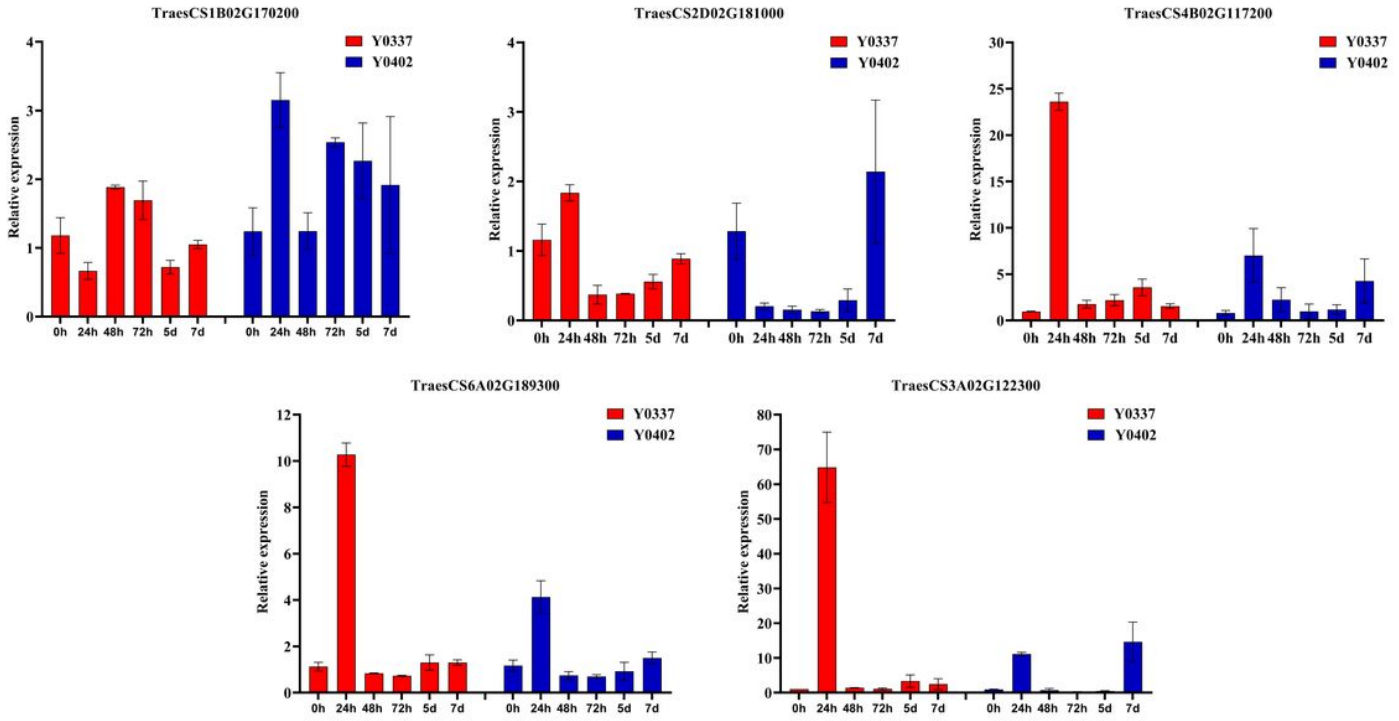

Figure 7

Expression patterns of five candidate genes for wheat stripe rust resistance following inoculation of Y0377 and Y0402 with *Pst*.

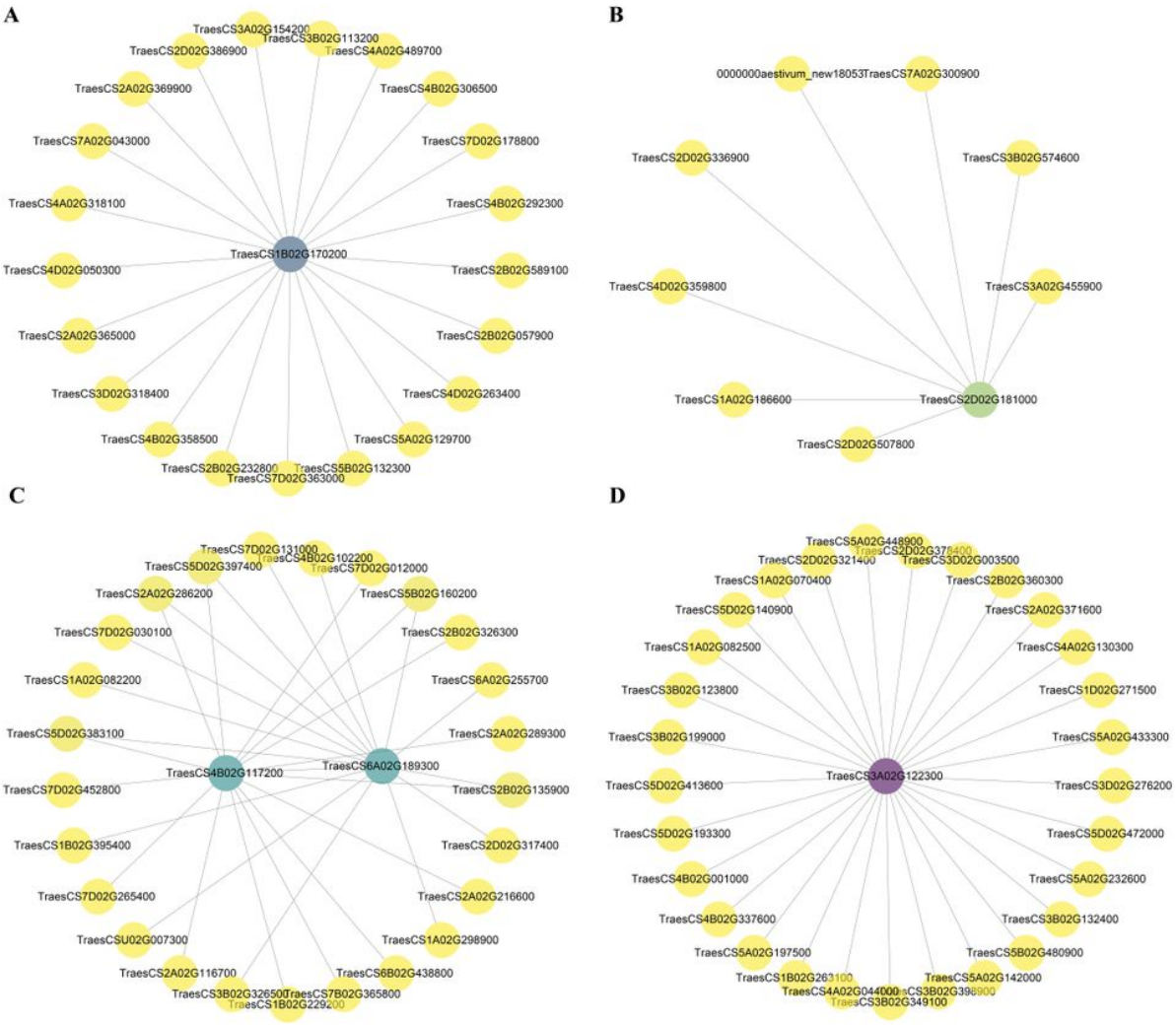

Figure 8

Gene co-expression networks. (A) Y0337 in the Red module. (B) Y0337 in the Yellowgreen module. (C) Y0337 in the Turquoise module. (D) Y0402 in the Darkgreen module.

Supplementary Files

This is a list of supplementary files associated with this preprint. Click to download.

- supplementarytablesS1S6.xlsx
- SupplementalFigureS1.jpg
- SupplementalFigureS2.jpg
- SupplementalFigureS3.jpg
- SupplementalFigureS4.jpg
- SupplementalFigureS5.jpg
- SupplementalFigureS6.jpg
- SupplementalFigureS7.jpg